

Magnetic bubbles in FePt nanodots with perpendicular anisotropy

C. Moutafis,¹ S. Komineas,^{1,2} C. A. F. Vaz,¹ J. A. C. Bland,¹ T. Shima,³ T. Seki,⁴ and K. Takanashi⁴

¹*Cavendish Laboratory, J. J. Thomson Avenue, Cambridge CB3 0HE, United Kingdom*

²*Max-Planck Institute for the Physics of Complex Systems, Nöthnitzer Strasse 38, 01187 Dresden, Germany*

³*Faculty of Engineering, Tohoku-Gakuin University, Tagajyo 985-8537, Japan*

⁴*Institute for Materials Research, Tohoku University, Sendai 980-8577, Japan*

(Received 1 February 2007; revised manuscript received 9 May 2007; published 24 September 2007)

We present experimental evidence, by magnetic force microscopy, for the existence of magnetic bubbles in suitably designed high-quality circular FePt nanodots. We specifically study dots of sizes where this fundamental magnetic state is a ground state and it is spontaneously created. We also observe triple-domain states consisting of concentric rings with alternating magnetization. A numerical study confirms the range of stability of the observed magnetic states and predicts the phase diagram in parameter space. Differences in the topology of these states imply distinct dynamical behavior, providing the basis for fundamental dynamical studies.

DOI: [10.1103/PhysRevB.76.104426](https://doi.org/10.1103/PhysRevB.76.104426)

PACS number(s): 75.60.Ch, 75.70.Kw, 75.75.+a

I. INTRODUCTION

Vortices are pervasive in nature, occurring in a variety of physical systems ranging from fluids and superfluids to superconductors and magnetic systems. Magnetic vortices are often formed and observed in circular disk elements with a weak in-plane magnetocrystalline anisotropy and arise due to the delicate interplay between the local energy terms and the long range dipole interaction confined by the circularly symmetric element edges. Both the detailed spin structure of this fundamental state¹⁻³ and the spin dynamics have been extensively studied experimentally and theoretically, including its characteristic dynamic modes of resonance^{4,5} and the gyro-tropic motion of the vortex core.⁶⁻¹² While the vortex is well understood both experimentally and theoretically as a fundamental state for magnetically soft circular disks, the question that arises is what is the corresponding fundamental state in the presence of a strong perpendicular anisotropy.

Experiments in hcp cobalt dots¹³ and in tetragonally distorted nickel dots,¹⁴ both of which have perpendicular anisotropies of similar strength (as measured by their quality factor), have often shown highly symmetric remanent states. Among the observed bidomain states are circular ones which are similar to magnetic bubbles. The same states were also reproduced and studied numerically.^{15,16} The stability of a bubble in a finite plate has been studied in Refs. 17 and 18 using an approximation of an infinitely sharp domain wall by calculations of the total force exerted on the wall. It was then argued that the bubble cannot be stabilized in very high anisotropy dots (in zero external field). In Ref. 19, disk-shaped particles with perpendicular anisotropy were studied numerically and theoretically, and it was shown that magnetic bubble states are the lowest energy states even in dots with a large perpendicular anisotropy, as in FePt dots. They are remanent states even in the absence of a bias field, which is in striking contrast to the magnetic bubbles observed in continuous films with perpendicular anisotropy.^{20,21} The non-trivial structure of their magnetization was pointed out, and their behavior under an external field was studied. Recent developments in the fabrication of magnetic elements based on FePt and CoPt binary alloys in the tetragonal $L1_0$ phase

have now made possible the study of the equilibrium states of magnetic dots with very strong perpendicular anisotropy.²²⁻²⁵ These have a uniaxial anisotropy which is one order of magnitude larger than that in materials used in previous studies.^{13,14} In this paper, we present experimental evidence for the existence of magnetic bubble states in FePt dots by magnetic force microscopy (MFM) imaging of arrays of dots with various diameters. In particular, we observe circular magnetic “bubbles” confined in the center of the dots as the most common bidomain state in sufficiently small dots. Whereas for the larger dots we see random labyrinthine magnetic patterns, we pinpoint the specific regime (diameter and thickness) where the bubble domain is manifested. We argue that this state is the analog of the vortex structure in the present high perpendicular anisotropy system. In particular, the domain wall around the observed bubbles should present a circulation directly corresponding to that of a vortex in isotropic dots. We also observe tridomain states which have the form of concentric rings with alternating magnetization. Similar states were observed in the experiments of Ref. 13. They can be interpreted as higher order bubble states. Our analysis indicates that perpendicular anisotropy dots can be used to significantly widen the scope for dynamical experiments in ferromagnetic elements beyond the current work on vortex dynamics.

II. EXPERIMENTAL METHODS AND RESULTS

Films of FePt in the tetragonal $L1_0$ phase have been patterned into arrays of circular dots. Thin films were prepared using an UHV magnetron sputtering apparatus. An Fe seed layer 1 nm thick and a 40 nm thick Au(001) buffer layer were first deposited on MgO(001) single crystal substrates at room temperature, followed by a 50 nm thick FePt(001) layer epitaxially grown on the Au buffer layer at 300 °C. The film composition was determined to be Fe₃₈Pt₆₂ by electron probe x-ray microanalysis. The dot arrays were fabricated using electron beam lithography and Ar ion milling.²² We have produced arrays of dots with lateral sizes $D=0.5, 1, 2,$ and $5 \mu\text{m}$. The spacing between the dots is approximately equal to their lateral size, and we assume that the dots are

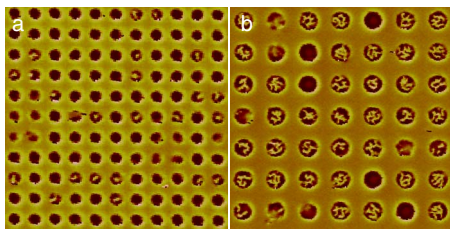


FIG. 1. (Color online) MFM images of $D=0.5 \mu\text{m}$ and $D=1 \mu\text{m}$ diameter dots. (a) The majority of the $D=0.5 \mu\text{m}$ dots are in a single-domain state; approximately 15% of them are in a bidomain state (most of the latter are in a monobubble). (b) The majority of the $D=1 \mu\text{m}$ dots are in a bidomain or tridomain state and a few are single domain.

only weakly interacting. Atomic force microscopy (AFM) and scanning electron microscopy (SEM) measurements were performed in order to check the quality of the dots. Larger dots are close to perfect disks with relatively sharp edges, while the edges of smaller dots are less sharp. Structural characterization of the patterned dots was performed by x-ray diffraction. It confirmed the existence of the FePt 001 and 003 superlattice peaks that indicate the formation of the $L1_0$ phase,²² which gives rise to the large uniaxial magnetocrystalline anisotropy. Magnetic properties were checked by a superconducting quantum interference device magnetometer. The anisotropy energy was found to be $K=3.0 \times 10^7 \text{ erg/cm}^3$ and the saturation magnetization $M_0=1100 \text{ emu/cm}^3$.

MFM measurements were performed in order to determine the remanent equilibrium states of the dot elements. This is a well established magnetic imaging technique which gives a measure of the vertical component of the stray field ensuing from the dot and is thus particularly well suited for the present studies of the magnetic domain structure of perpendicular anisotropy elements. A Digital Instruments (Veeco Metrology Group) DimensionTM 3100 with a Nanoscope IV controller was used in Tapping and Lift modeTM, which allows the imaging of topography and magnetic information in a single scan.²⁶ We used CoCr-coated silicon tips magnetized along the tip axis (perpendicular to the sample surface).

We initially saturated the dot arrays by applying a large perpendicular field. For the $D=5$ and $2 \mu\text{m}$ diameter dots, the remanent state consists of random labyrinth-like domains. The crossover from simple structures to labyrinthine domains was previously observed in Refs. 13 and 14. The domain structure in this case is, thus, similar to that in continuous films. However, the effects of the finite geometry manifest themselves clearly in the smaller dots, where we observe the emergence of a markedly different behavior. For the $D=1$ and $0.5 \mu\text{m}$ dots, highly symmetric magnetic states are observed. An estimate of the abundance of these axially symmetric states can be drawn from overview MFM images shown in Fig. 1.

For the $D=0.5 \mu\text{m}$ dot array shown in Fig. 1(a), most of the dots are in a single-domain state, but a significant number of them adopt a bidomain state of striking simplicity. The interplay between the magnetic energy terms—exchange, an-

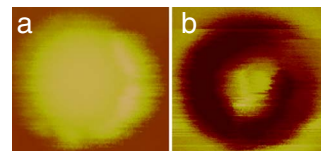


FIG. 2. (Color online) (a) The topography (AFM image) of a $D=0.5 \mu\text{m}$ FePt dot. (b) The magnetic contrast image (MFM) of the same dot shows the signature of an almost axially symmetric monobubble in the center of the dot.

isotropy, and demagnetizing energy—leads, in this case, to the emergence of a highly symmetric magnetic state. An example of a dot in such a state is shown in Fig. 2. The center of the dot is occupied by a circular magnetic domain which resembles the magnetic bubbles, which are observed in ferromagnetic films with perpendicular anisotropy in the presence of a bias field.²⁰ We call this bidomain state, containing one circular bubble in the center of the dot, the “monobubble” state. We note that the shape of the dots is not perfectly circular. In particular, we could easily identify rough edges in the AFM and SEM images. Therefore, the present results show that the bubble state is robust against shape imperfections and variations in the dot geometry.

In Ref. 19, magnetic bubbles were studied as equilibrium states in high perpendicular anisotropy particles. It was noted that these fundamental states share important features with vortices, which are the most common magnetic structures in low anisotropy particles. In particular, the domain wall around the bubble presents a circulation which assigns to the whole magnetic structure a nontrivial topological number. A magnetic bubble was found to have lower energy than the single-domain state for particles of sufficiently large lateral dimensions, and it was predicted that this should be the ground state for a wide range of dot diameters in strong perpendicular anisotropy dots. The present results confirm, to a large extent, the theoretical predictions. A more complete account of the theory adjusted for the parameters of the present particles is given below.

Figure 1(b) shows that some of the $D=1 \mu\text{m}$ dots are in the remanent single-domain state. This state should be metastable as shown in numerical calculations presented later in this paper. However, most of the dots have small domains of opposite magnetizations with an irregular serpentine shape, which are usually confined to the interior of the dot. These magnetic domains often have the shape of a curved stripe, and the domain structure is best described as a bidomain or a tridomain state. Symmetrical domain structures are possible at these dot sizes, and almost concentric tridomain ring structures are indeed observed in some dots, as shown in Fig. 3(b). These regular patterns are important for the understanding of the domain structure, as we will discuss later when we present our numerical results. A similar type of domain structure was observed in continuous films²⁷ and was termed the hollow bubble. It was shown to be stable only for a very small range of applied fields. In Fig. 3(c), we observed a state where, in contrast to the usually observed behavior, the domains have not fully branched out and are localized in the center, giving rise to a two-domain state. The domain walls

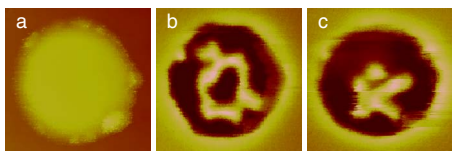


FIG. 3. (Color online) AFM and MFM images of $D=1 \mu\text{m}$ dots. (a) Topography (AFM) of a dot. (b) A MFM signal which reveals a ringlike structure indicating three almost concentric magnetic domains of alternating magnetization. (c) In contrast to the concentric structure in (b) and to the usual behavior observed, an irregularly shaped domain is localized in the center and has not branched out.

are not smooth, probably because the domain wall coercivity plays an important role. We find that in both the 1 and $0.5 \mu\text{m}$ diameter dots, the domains are mostly localized away from the dot boundary. A further extensive study of dots with different geometrical features would be required to study whether this interesting feature persists.

III. NUMERICAL RESULTS AND DISCUSSION

In order to analyze the experimental findings and gain insight into the magnetization distributions that give rise to the observed MFM pictures, we have performed a detailed numerical study based on the Landau-Lifshitz equation. Following Ref. 19, we have calculated numerically the energetics of axially symmetric magnetic states in a single disk-shaped particle using a numerical code which exploits the axial symmetry.²⁸ For the FePt dots used in our experiments, we assume an exchange length $\ell_{ex}=4.0 \text{ nm}$ and a quality factor $Q=4.7$. The latter is defined as $Q \equiv K/2\pi M_0^2$, where K is the uniaxial anisotropy constant. We use here an on-site anisotropy. We consider a disk of thickness $t=12.5\ell_{ex}(=50 \text{ nm})$ and a diameter in the range $30\ell_{ex} < D < 200\ell_{ex}$ (or $120 \text{ nm} < D < 800 \text{ nm}$).

We find the equilibrium magnetization configuration and the corresponding energies for the single-domain state and cylindrically symmetric bidomain and tridomain states, which are shown in Fig. 4. The energy of the single-domain state as a function of dot radius (R) is denoted by a dotted line. The bidomain state (solid line) corresponds to the monobubbles observed in our experiments. It exists for $R > 24\ell_{ex}$, and its energy is lower than the energy for a single domain for $R > R_{c1}=30\ell_{ex}$. For the present case of high anisotropy ($Q > 1$), the bubble exists as a metastable state for large diameters. The corresponding state is unstable in dots with $Q < 1$ (Ref. 14) for larger diameters.²⁹

The domain wall is Bloch near the central plane, and it progressively becomes Néel like toward the top and bottom surfaces. This structure has been discussed in the literature,³⁰ and we find this structure even for materials with a very large anisotropy such as FePt. A plot of the magnetization vector at the top surface of the monobubble state is given in Fig. 5. The figure presents numerically calculated data, but it is designed to give only a simplified illustration of the bubble. It shows the spatial variation of the magnetization from “up” to “down” across the dot radius, and also the winding of the magnetization vector around the axis of the dot. Numerical

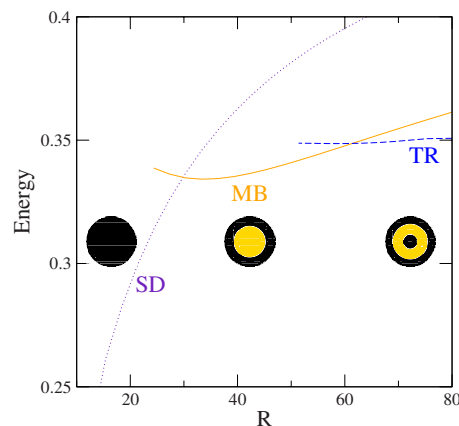


FIG. 4. (Color online) Energy per unit volume (in units of $2\pi M_0^2$) as a function of the particle radius R (in units of ℓ_{ex}) for the single domain (SD, dotted line), the monobubble (MB, solid line), and the three-ring (TR, dashed line) state. The dot thickness is $t=12.5\ell_{ex}$ and the quality factor $Q=4.7$. The intersection between the dotted and solid lines corresponds to R_{c1} , while the one between the solid and dashed lines corresponds to R_{c2} (see text). The insets represent calculated profiles of the perpendicular magnetization for the three states. The color contrast indicates domains of antiparallel magnetization.

data show that the domain wall is relatively sharp. In contrast, the domain wall of bidomain states in cobalt¹³ and nickel¹⁴ dots is not localized but extends over the dot radius.²⁹ The important difference with the material studied in the present paper is that cobalt and nickel have a quality factor $Q \approx 0.4$, which is less than unity, and thus, the anisotropy is weaker than the magnetostatic field. In conclusion, bubbles exist for a wide range of quality factors, but their detailed features do depend on the quality factor. These features, e.g., the width of the domain wall, could be of crucial importance for their dynamical properties.

A tridomain state of axial symmetry has the form of concentric rings with alternating magnetization and we will call this a three-ring state. Its energy as a function of the dot radius is given in Fig. 4 (dashed line). It exists for $R > 51\ell_{ex}$ and has lower energy than the monobubble for $R > R_{c2}=61.5\ell_{ex}$. In fact, the radius $R=R_{c2}$ corresponds approximately to $D=0.5 \mu\text{m}$, marking the crossover between dot sizes where the three-ring states become energetically

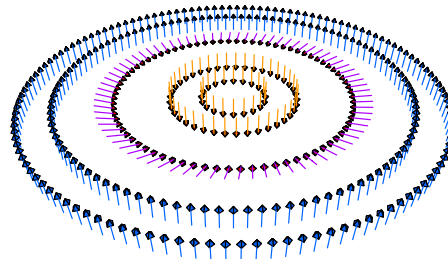


FIG. 5. (Color online) Magnetization vector at the top surface of a dot in the monobubble state. The inner “down” and the outer “up” domains as well as the Néel-like domain wall in between are illustrated.

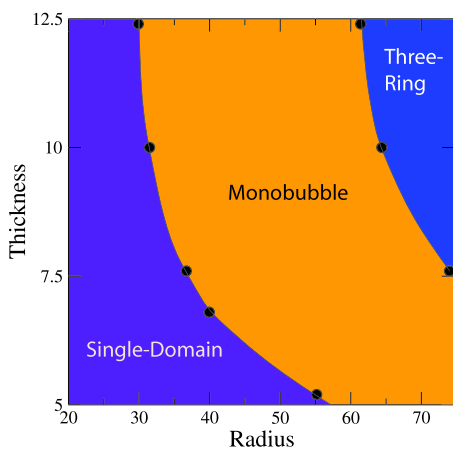


FIG. 6. (Color online) Phase diagram for varying dot thickness t and radius R (both in units of ℓ_{ex}). The regimes where the single domain, the monobubble, and the three-ring states are energetically favorable are indicated. We vary the thickness in the range $5\ell_{\text{ex}} < t < 12.5\ell_{\text{ex}}$ (or $20 \text{ nm} < t < 50 \text{ nm}$). The lines correspond to R_{c1} and R_{c2} as a function of t (see Fig. 4). The numerically calculated points are indicated by circles.

favorable, in good agreement with our observations. Higher order multidomain states of axial symmetry could be present in larger dots, and they would have the form of multiple concentric rings with alternating magnetization.¹³ However, the increasing complexity of the magnetic energy landscape in larger dots is expected to make the observation of such concentric domain states less probable. Instead, the stripe domains should dominate as discussed extensively in the literature.³⁰ In fact, the observation of random labyrinth domain patterns in the larger dots seems to suggest that above a certain diameter, the domain configuration is not influenced significantly by the size of the element. We also present, in Fig. 6, a numerical phase diagram in parameter space. Only axially symmetric states are presented in this figure. The monobubble is stable over a wide range of parameter values. For thinner dots the monobubble is stable only for larger dot diameters. The stability of concentric ring domains in cylindrical samples under perpendicular applied fields was theoretically described in Ref. 18 using an approximation of an infinitely sharp domain wall.

We return to the detailed magnetization configurations of multidomain states and note that their complexity can be quantified by a topological invariant which is often called the “Skyrmion number.” We define $\mathbf{m} \equiv \mathbf{M}/M_s$, where \mathbf{M} is the magnetization vector and M_s is the saturation magnetization. Then we define $\mathcal{N} \equiv 1/(4\pi)\epsilon_{\mu\nu}\int(\partial_\nu\mathbf{m} \times \partial_\mu\mathbf{m}) \cdot \mathbf{m}d^2x$, where $\epsilon_{\mu\nu}$ is the antisymmetric tensor. The integration extends over a plane, e.g., over the top plane of a film. This is a topologi-

cal invariant which takes integer values in the case of an infinite two-dimensional medium (continuous magnetic films), and it does not depend on the chosen plane of integration. In the case of axially symmetric configurations, the formula for \mathcal{N} assumes a simple form²⁸ and it is easy to find that the single domain has $\mathcal{N} \approx 0$ and the monobubble has $\mathcal{N} \approx \pm 1$. The sign for \mathcal{N} depends on the bubble “polarity” (orientation of the magnetization at the dot center). A vortex, such as those observed in dots, has $\mathcal{N} = \pm 1/2$, where the sign depends on the vortex polarity.³¹ The magnetization vector winds one full circle as we move around the vortex core and, thus, the vortex is the simplest topologically nontrivial structure in soft dots. The same winding of the magnetization is present at the domain wall of the monobubble (see Fig. 5), and the latter is the simplest topologically nontrivial structure in magnetically hard dots. Due to its half-integer Skyrmion number, a vortex can be viewed as a “half bubble” or a “meron” (the latter term was introduced in Ref. 32). For the three-ring states studied in this paper, we find $\mathcal{N} \approx 0$. Three-ring states with $\mathcal{N} \neq 0$ would include domain walls with negative or multiple windings. They will not be mentioned further here as we do not expect that such states are practically possible to realize.

The topological number \mathcal{N} is directly linked to the magnetization dynamics since it is proportional to the gyrocoupling vector,³³ while its value has implications for the conservation laws of the Landau-Lifshitz equation.²⁸ In particular, the dynamics for $\mathcal{N}=0$ differs qualitatively from that for $\mathcal{N} \neq 0$. The number \mathcal{N} takes into account also the polarity, and vortices with different values of \mathcal{N} have different dynamical behaviors. The profound effect of the polarity on vortex dynamics has been experimentally demonstrated in Refs. 10 and 11. The same effect is expected for the dynamics of the monobubble. Furthermore, the above considerations imply a qualitative difference between the dynamics of a monobubble and that of a three-ring state. This difference should be manifested, e.g., in the excitation spectrum³⁴ and in the magnetization profile motion under the influence of an external field gradient. Thus, our observations and the analysis provide the basis for a much wider scope for dynamical experiments in ferromagnetic elements compared to currently investigated vortex dynamics phenomena.

ACKNOWLEDGMENTS

C.M. is grateful to Wen-Siang Lew for help with the AFM. C.M. was supported by the Cambridge European Trust, Emmanuel College (Cambridge, UK), and Cambridge Philosophical Society. S.K. was supported by EPSRC Grant No. GR/S61263/01. This work was supported by the EPSRC (UK).

- ¹T. Shinjo, T. Okuno, R. Hassdorf, K. Shigeto, and T. Ono, *Science* **289**, 930 (2000).
- ²A. Wachowiak, J. Wiebe, M. Bode, O. Pietzsch, M. Morgenstern, and R. Wiesendanger, *Science* **298**, 577 (2002).
- ³J. Raabe, R. Pulwey, R. Sattler, T. Schweinböck, J. Zweck, and D. Weiss, *J. Appl. Phys.* **88**, 4437 (2000).
- ⁴M. Buess, R. Höllinger, T. Haug, K. Perzlmaier, U. Krey, D. Pescia, M. R. Scheinfein, D. Weiss, and C. H. Back, *Phys. Rev. Lett.* **93**, 077207 (2004).
- ⁵M. Buess, T. P. J. Knowles, R. Höllinger, T. Haug, U. Krey, D. Weiss, D. Pescia, M. R. Scheinfein, and C. H. Back, *Phys. Rev. B* **71**, 104415 (2005).
- ⁶D. L. Huber, *Phys. Rev. B* **26**, 3758 (1982).
- ⁷K. Yu. Guslienko, B. A. Ivanov, V. Novosad, Y. Otani, H. Shima, and K. Fukamichi, *J. Appl. Phys.* **91**, 8037 (2002).
- ⁸N. A. Usov and L. G. Kurkina, *J. Magn. Magn. Mater.* **242–245**, 1005 (2002).
- ⁹J. P. Park, P. Eames, D. M. Engebretson, J. Berezovsky, and P. A. Crowell, *Phys. Rev. B* **67**, 020403(R) (2003).
- ¹⁰S. B. Choe, Y. Acremann, A. Scholl, A. Bauer, A. Doran, J. Stöhr, and H. A. Padmore, *Science* **304**, 420 (2004).
- ¹¹K. S. Buchanan, P. E. Roy, M. Grimsditch, F. Y. Fradin, K. Yu. Guslienko, S. D. Bader, and V. Novosad, *Nat. Phys.* **1**, 172 (2005).
- ¹²D. D. Sheka, J. P. Zagorodny, J.-G. Caputo, Y. Gaididei, and F. G. Mertens, *Phys. Rev. B* **71**, 134420 (2005).
- ¹³M. Hehn, K. Ounadjela, J.-P. Bucher, F. Rousseaux, D. Decanini, B. Barteliani, and C. Chappert, *Science* **272**, 1782 (1996).
- ¹⁴G. D. Skidmore, A. Kunz, C. E. Campbell, and E. D. Dahlberg, *Phys. Rev. B* **70**, 012410 (2004).
- ¹⁵L. D. Buda, I. L. Prejbeanu, M. Demand, U. Ebels, and K. Ounadjela, *IEEE Trans. Magn.* **37**, 2061 (2001).
- ¹⁶J. Kin Ha, R. Hertel, and J. Kirschner, *Europhys. Lett.* **64**, 810 (2003).
- ¹⁷W. F. Druyvesteyn, R. Szymczak, and R. Wadas, *Phys. Status Solidi A* **9**, 343 (1972).
- ¹⁸V. A. Ignatchenko and E. Yu. Mironov, *J. Magn. Magn. Mater.* **124**, 315 (1993).
- ¹⁹S. Komineas, C. A. F. Vaz, J. A. C. Bland, and N. Papanicolaou, *Phys. Rev. B* **71**, 060405(R) (2005).
- ²⁰A. P. Malozemoff and J. C. Slonczewski, *Magnetic Domain Walls in Bubble Materials* (Academic, New York, 1979).
- ²¹A. A. Thiele, *J. Appl. Phys.* **41**, 1139 (1970).
- ²²T. Seki, T. Shima, K. Yakushiji, K. Takanashi, G. Q. Li, and S. Ishio, *IEEE Trans. Magn.* **41**, 3604 (2005).
- ²³M. Abes, M. V. Rastei, J. Vénuat, L. D. Buda-Prejbeanu, A. Carvalho, G. Schmerber, J. Arabski, E. Beaurepaire, J. P. Bucher, A. Dinia, and V. Pierron-Bohnes, *Mater. Sci. Eng., B* **126**, 207 (2006).
- ²⁴S. E. Russek and W. E. Bailey, *IEEE Trans. Magn.* **36**, 2990 (2000).
- ²⁵O. Kazakova, M. Hanson, and E. B. Svedberg, *IEEE Trans. Magn.* **39**, 2747 (2003).
- ²⁶*Dimension™ 3100 Manual*, Veeco Metrology Group, Digital Instruments.
- ²⁷F. A. De Jonge, W. F. Druyvesteyn, and A. G. H. Verhulst, *J. Appl. Phys.* **42**, 1270 (1971).
- ²⁸S. Komineas and N. Papanicolaou, *Physica D* **99**, 81 (1996).
- ²⁹C. Moutafis, S. Komineas, C. A. F. Vaz, J. A. C. Bland, and P. Eames, *Phys. Rev. B* **74**, 214406 (2006).
- ³⁰A. Hubert and R. Schäfer, *Magnetic Domains* (Springer, Berlin, 1998).
- ³¹The topological number \mathcal{N} discussed here does not coincide with the “winding number” very often used in the literature on vortices. The winding number takes nonzero integer values for vortices and it does not depend on the vortex polarity. The number \mathcal{N} does depend on the magnetization vector winding, but it also depends on the out-of-plane magnetization component.
- ³²D. J. Gross, *Nucl. Phys. B* **132**, 439 (1978).
- ³³A. A. Thiele, *Phys. Rev. Lett.* **30**, 230 (1973).
- ³⁴N. Vukadinovic and F. Boust, *Phys. Rev. B* **75**, 014420 (2007).